

Heusler-alloy-based CPP-GMR devices with high MR outputs

K. Hono

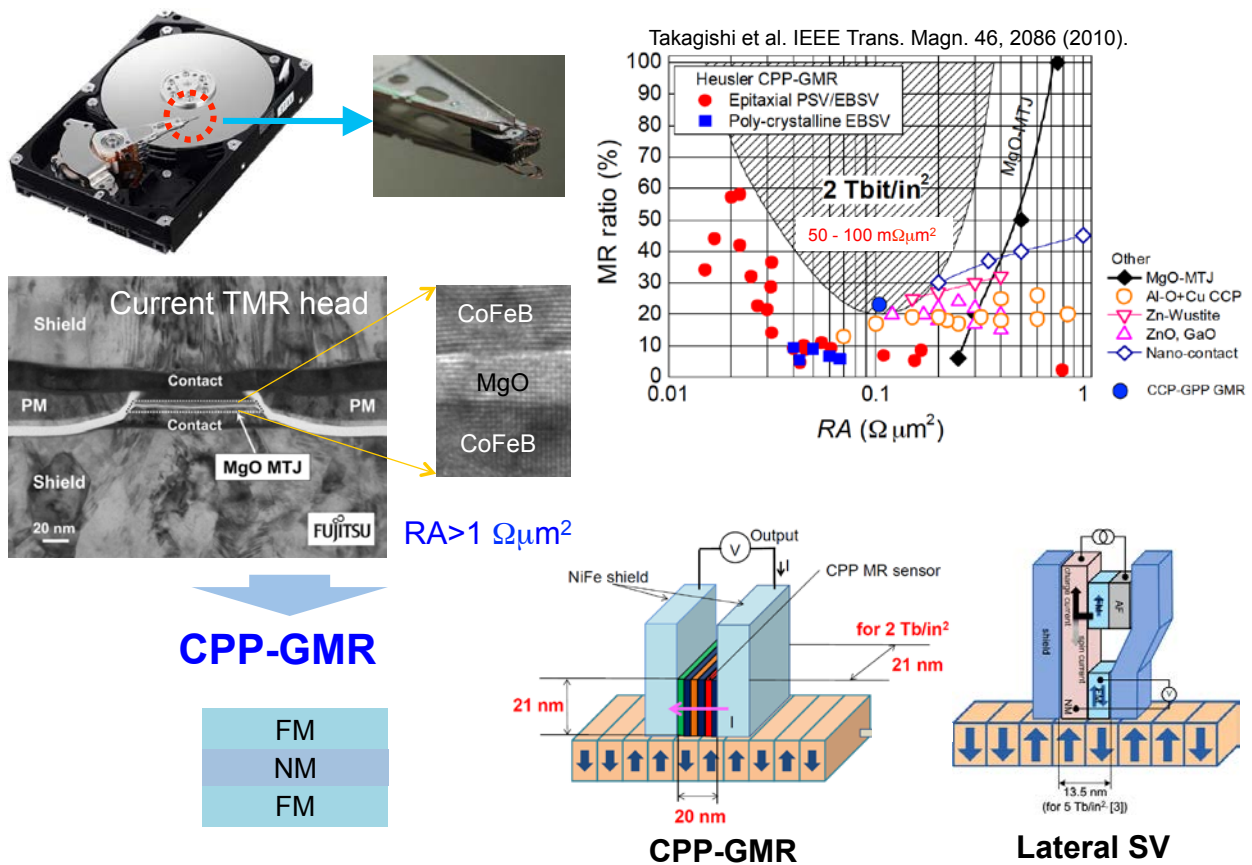
*Magnetic Materials Unit
National Institute for Materials Science (NIMS)
Tsukuba 305-0047, Japan*

Collaborators

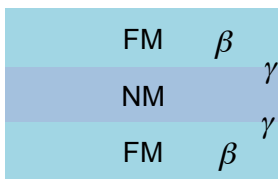
T. Furubayashi, Y. Sakuraba, Y. K. Takahashi
S. T. Li, J. Chen, Du Ye, T. T. Sasaki

<http://www.nims.go.jp/mmu/>

Read head for >2 Tbit/in²



CPP-GMR and FM Heusler alloys



$$\Delta RA \approx 2\rho_F \frac{\beta^2}{1-\beta^2} t_F + 4AR_{F/N} \frac{\gamma^2}{1-\gamma^2}$$

For 1 Tb/in²

MR ~ 10-20%

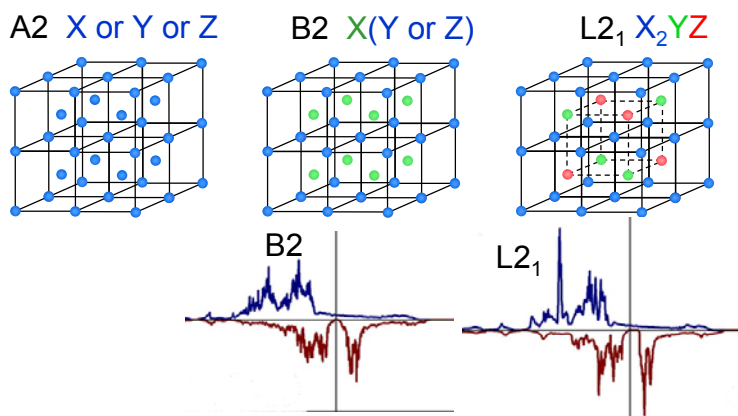
$$\Delta V = \Delta RA \times J = MR\% \times V_{BIAS} > 12 \text{ mV}$$

12% MR & J ~ $2 \times 10^8 \text{ A/cm}^2$

High damping against J

after Jeff Childress, HGST

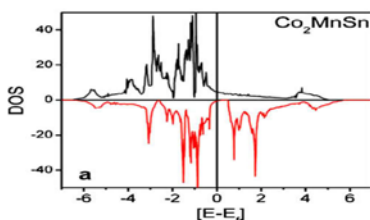
Co₂FeZ or Co₂MnZ Heusler alloys



Search for highly spinpolarized FM alloys

DOS calculation

DOS calculations: VASP



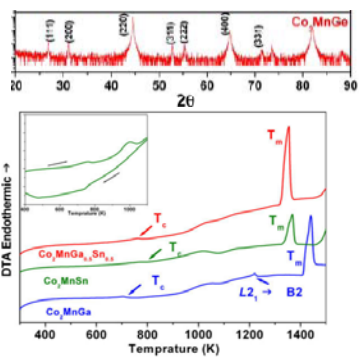
Alloy preparation

arc melting or induction meting



+ annealing

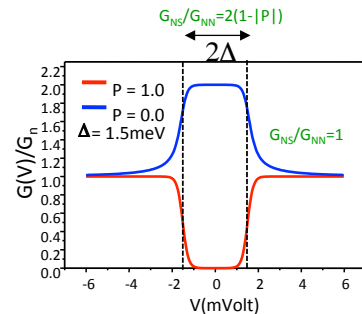
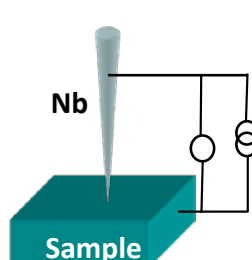
XRD & Thermal analysis



T_c, order-disorder temperature, melting point

Spin polarization

Point Contact Andreev Reflection (PCAR)



Conductance-bias

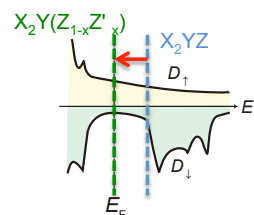
Spin polarization measured by PCAR

Quaternary alloys	P(%)	Ref.
Co ₂ Mn(Ge _{0.75} Ga _{0.25})	74	1
Co ₂ Mn(Ga _{0.5} Sn _{0.5})	72	2
Co ₂ Fe(Si _{0.75} Ge _{0.25})	70	3
Co ₂ Fe(Ga _{0.5} Ge _{0.5})	68	4
Co ₂ (Cr _{0.02} Fe _{0.98})Ga	67	5
Co ₂ Mn(GeSn)	67	6
Co ₂ (Mn _{0.95} Fe _{0.05})Sn	65	7
(Co, Fe) ₂ MnGe	65	8
Co ₂ (Mn _{0.5} Fe _{0.5})Ga	65	9
Co ₂ (Cr _{0.02} Fe _{0.98})Si	65	10
Co ₂ Mn(Ti,Sn)	64	11
Co ₂ Mn(Al _{0.5} Sn _{0.5})	63	12
Co ₂ Mn(Ga _x Si _{1-x})	63	13
Co ₂ Fe(Al,Ga)	63	14
Co ₂ Mn(SiGe)	63	15
Co ₂ (Mn _{0.5} Fe _{0.5})Si	61	16
Co ₂ (Cr,Fe)Al	60	17
Co ₂ Mn(Al _{0.5} Si _{0.5})	60	18
Co ₂ Fe(Ga _{0.5} Si _{0.5})	60	19
Co ₂ Fe(Al _{0.5} Si _{0.5})	60	20

Ternary alloys	P	Ref.
Co ₂ MnSi	56	21
Co ₂ MnGe	58	1
Co ₂ MnSn	60	12
Co ₂ MnAl	60	12
Co ₂ MnGa	60	1
Co ₂ CrAl	62	17
Co ₂ FeAl	59	17
Co ₂ FeSi	60	10
Co ₂ FeGa	58	22
Co ₂ CrGa	61	23
Co ₂ TiSn	57	24
Co ₂ VAI	48	25
Fe ₂ VAI	56	25

Metals and binary	P	Ref.
Fe	46	
Co	45	
FeCo	50	
Co ₇₅ Fe ₂₅	58	
B2-FeCo	60	
[Co/Pd] _n	60	
Fe ₄ N	59	26
Co/Pt	56	27

1. B. Varaprasad *et al.*, APEX3 023002 (2010).
2. B. Varaprasad *et al.*, Acta Mater. **57** 2702 (2009).
7. A. Rajanikanth *et al.*, JAP **103** 103904 (2008).
10. S.V. Karthik *et al.*, JAP **102** 043903 (2007).
12. A. Rajanikanth *et al.*, JAP **101** 09J508 (2007).
17. S.V. Karthik *et al.*, APL **89** 052505 (2006).
20. T.M. Nakatani *et al.*, JAP **102** 033916 (2007).
21. A. Rajanikanth *et al.*, JAP **105** 063916 (2009).
23. T.M. Nakatani *et al.*, JPD **41** 225002 (2008).
25. S.V. Karthik *et al.*, Acta Mater. **55** 3867 (2007).
26. A. Narahara *et al.*, APL **94** 202502 (2009).
27. A. Rajanikanth *et al.*, APL **97** 022505 (2010).
- 3-6, 8, 9, 11, 13-17, 18-20, 22, 24. To be submitted



V. Varaprasad et al. Acta Mater. (2012).

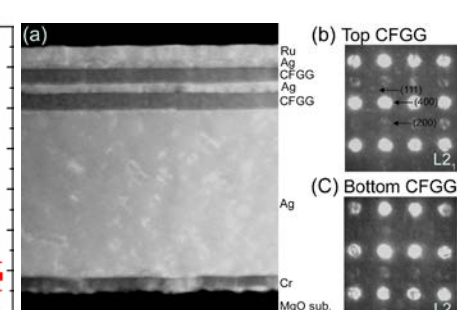
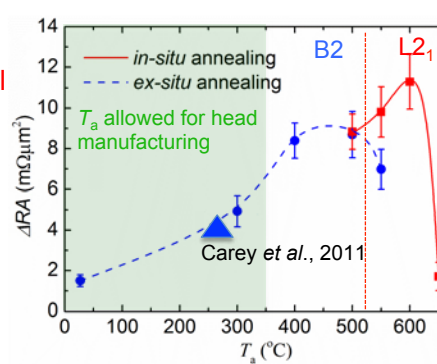
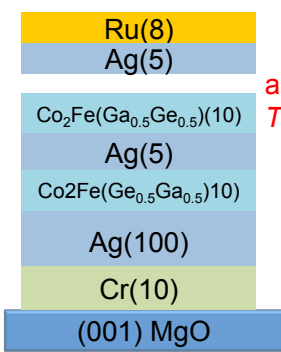
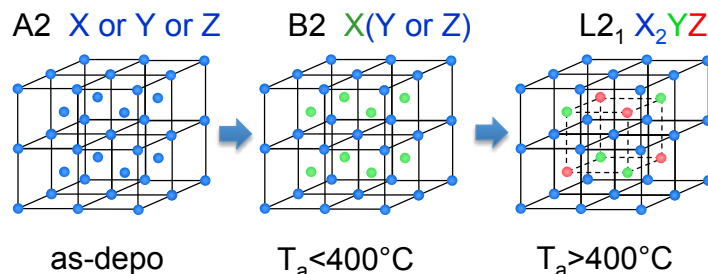
ΔRA increase by annealing

Co₂Fe(Ga_{0.5}Ge_{0.5})

B.S.D.Ch.S. Varaprasad et a. Acta Mater. 60, 6257 (2012).

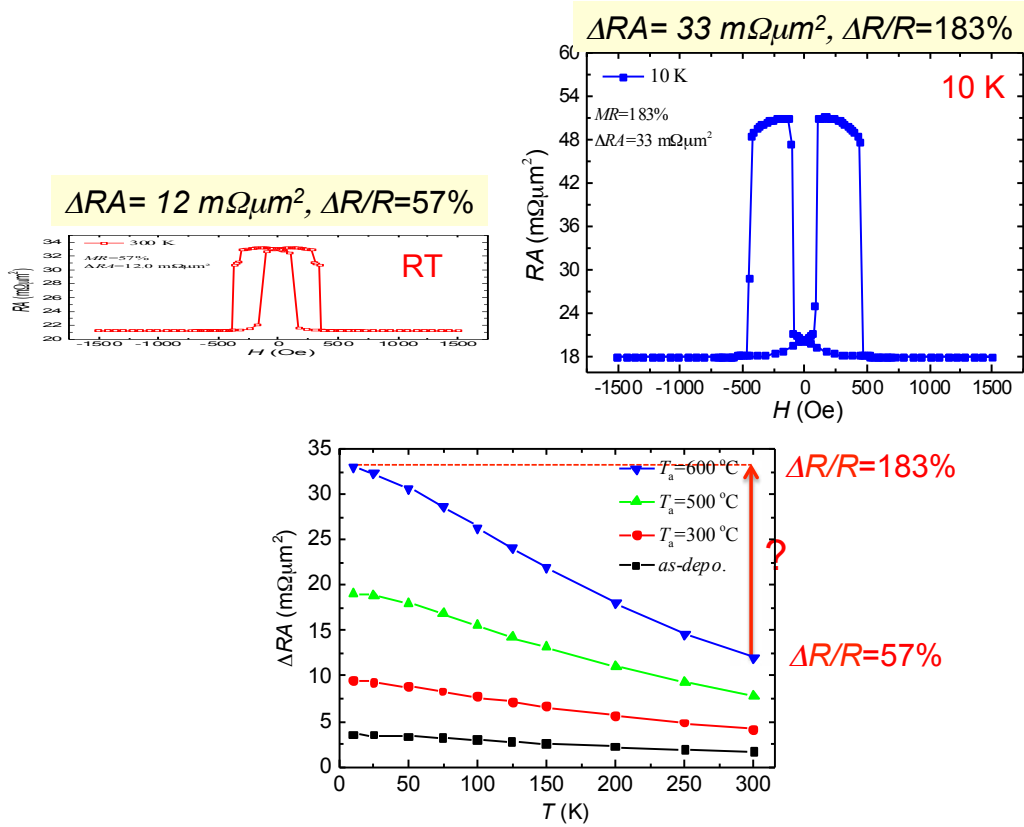


S. T. Li



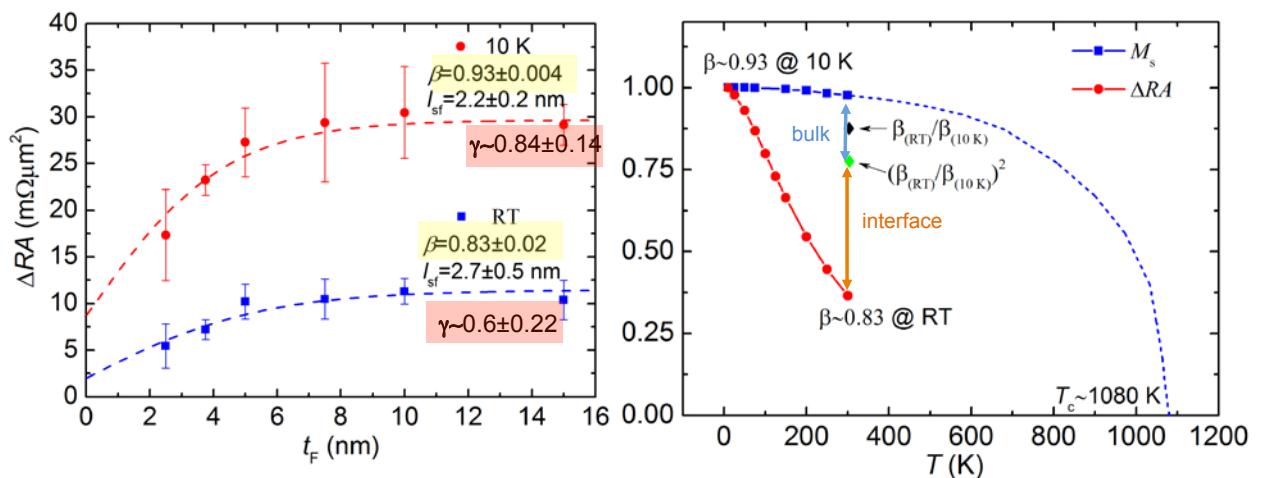
S. Li, Y.K. Takahashi, T. Furubayashi, and K. Hono, APL 103, 042405 (2013).

Large temperature dependence of MR



S. Li, Y.K. Takahashi, T. Furubayashi, and K. Hono, APL 103, 042405 (2013).

Origin of T dependence of ΔRA



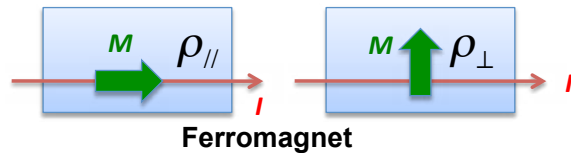
$$\Delta RA \approx 2\rho_F \frac{\beta^2}{1-\beta^2} t_F + 4AR_{F/N} \frac{\gamma^2}{1-\gamma^2}$$

Which contributes to T-dependence of ΔRA , β or γ ?

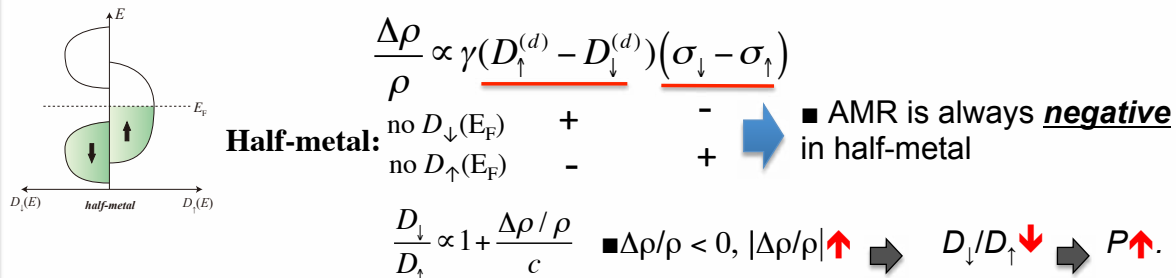
Eveluation of β using AMR measurements

Anisotropy magnetoresistance (AMR)

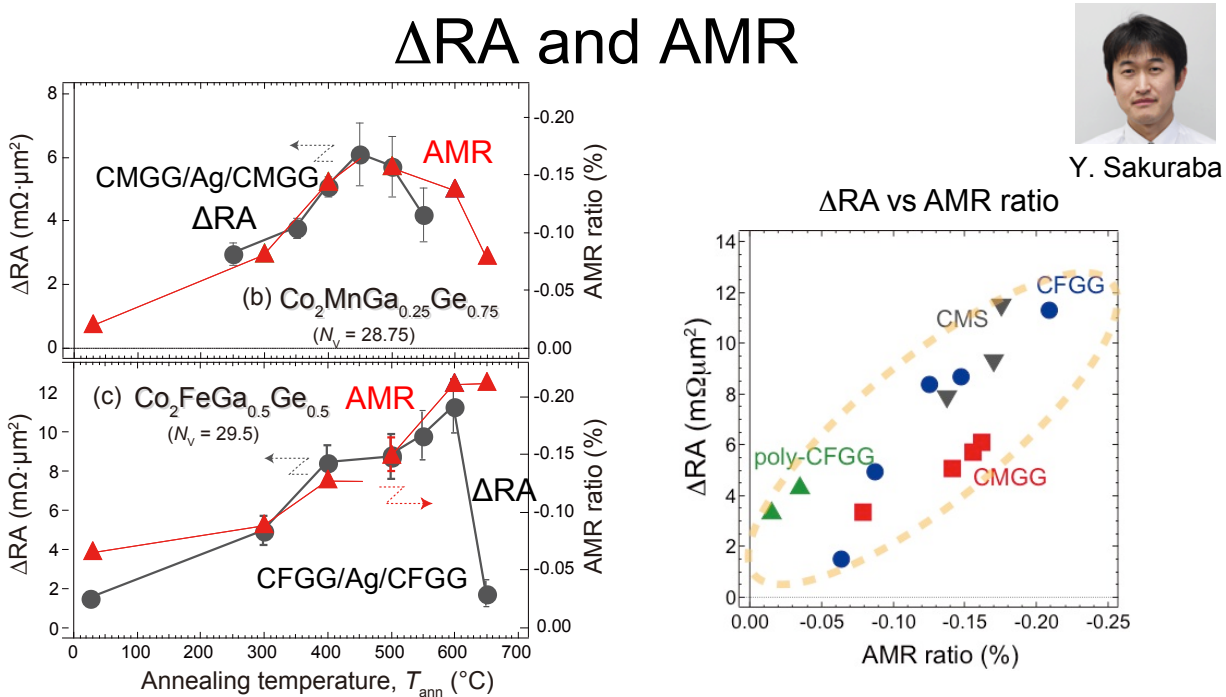
$$\frac{\Delta\rho}{\rho} = \frac{\rho_{\parallel} - \rho_{\perp}}{\rho_{\parallel}} \times 100(\%) \quad \begin{array}{l} \rho_{\parallel} > \rho_{\perp}: \text{Positive} \\ \rho_{\parallel} < \rho_{\perp}: \text{Negative} \end{array}$$



Theory of AMR and spin asymmetry by Kokado



Kokado et al. (J. Phys. Soc. Jpn. 81, 024705 (2012))



Excellent correlation between AMR and ΔRA

Facile way to estimate β

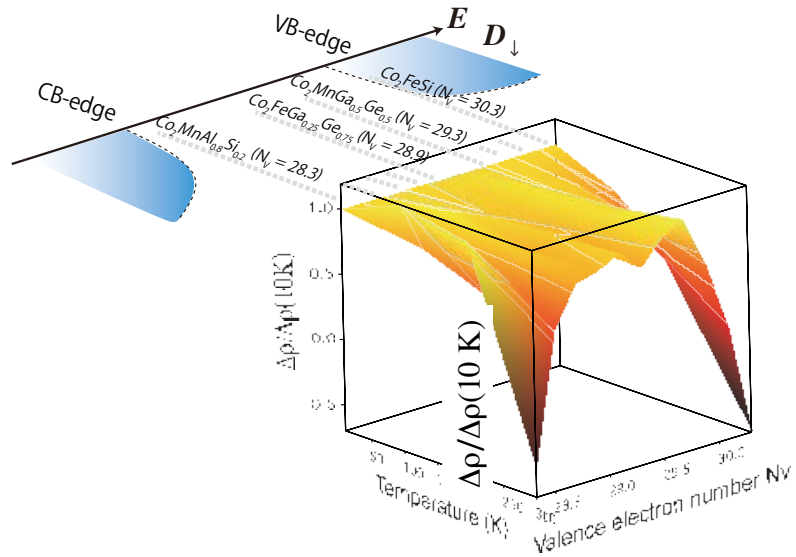
Y. Sakuraba et al. APL104, 172407 (2014).

Temperature dependence of $\Delta\rho$



Y. Sakuraba

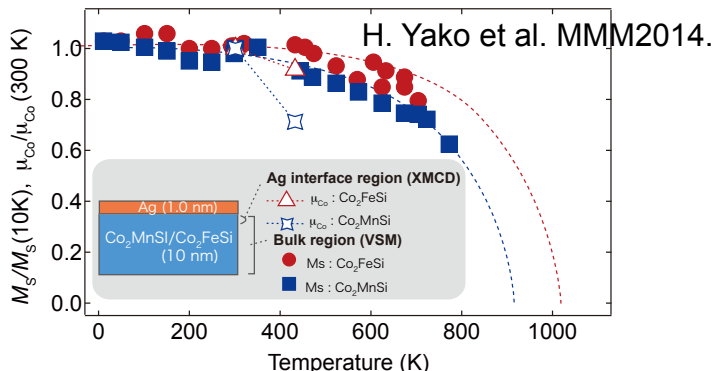
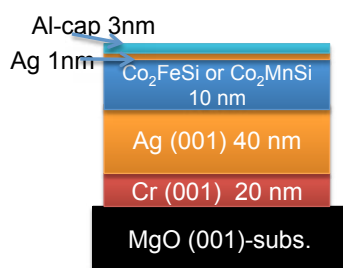
$$\Delta\rho(T) = \text{AMR}(T) \times \rho(T)$$



β of CFGG does not degrade at RT!

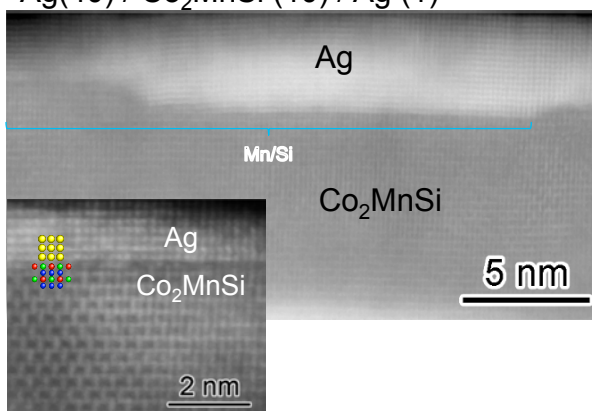
Y. Sakuraba et al. APL104, 172407 (2014).

T dependence of μ_{Co} at CMS & CFS/Ag interfaces

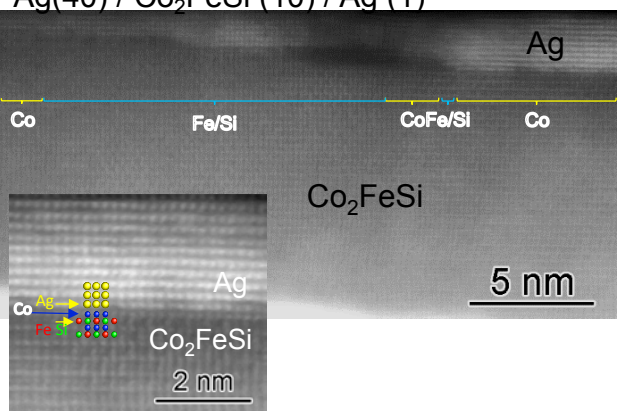


Y. Sakuraba

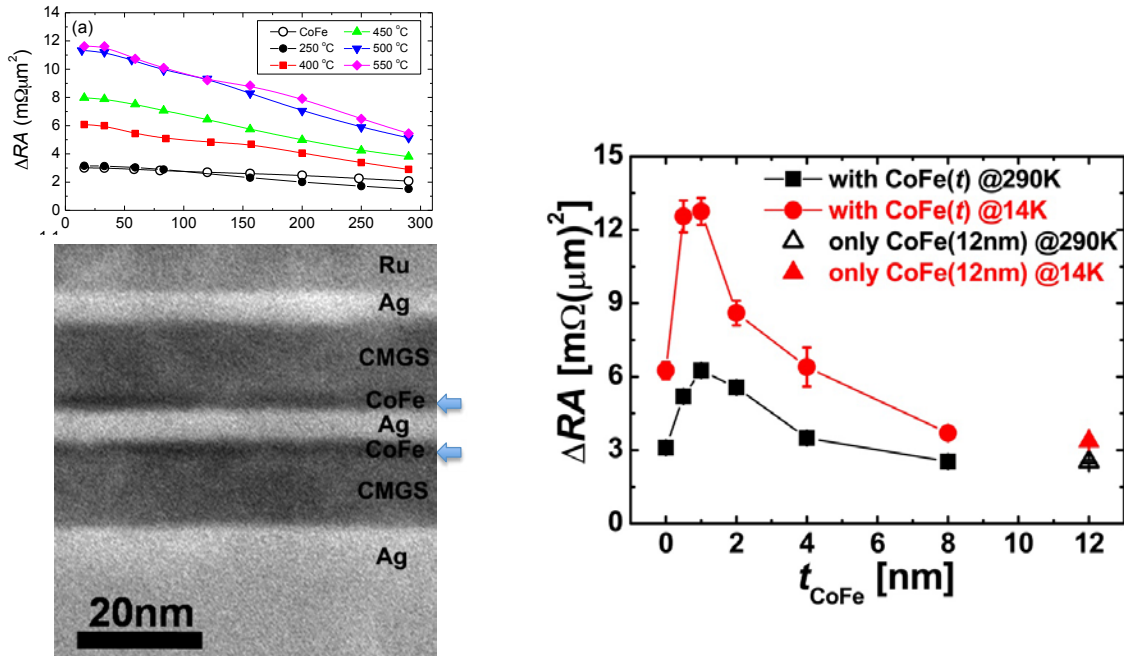
Ag(40) / Co₂MnSi (10) / Ag (1)



Ag(40) / Co₂FeSi (10) / Ag (1)



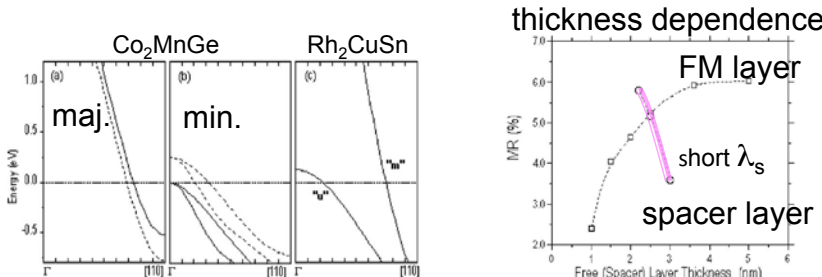
How to suppress the reduction of spin moment at Hesuer/Ag interface?



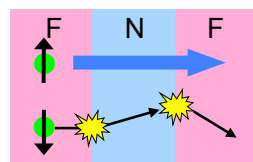
Inversion of thin FM layer for increasing exchange stiffness

N. Hase et al. JAP 109, 07E112 (2011).

Band matching at FM/NM interface



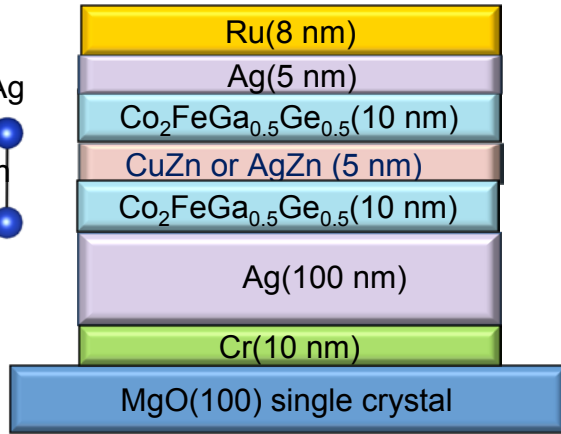
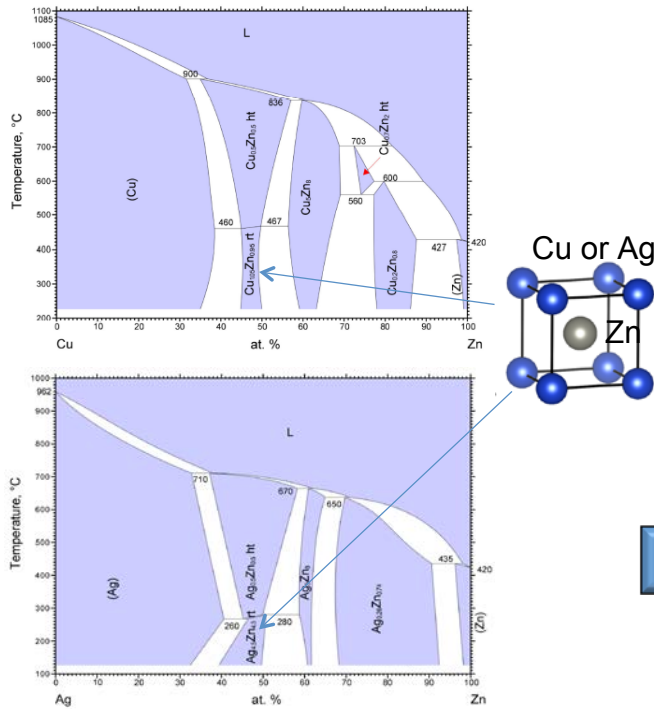
K. Nikolaev et al., Appl. Phys. Lett. 94, 222501(2009)



$$\Delta RA \propto AR_{F/N} \cdot \gamma^2 / (1 - \gamma^2)$$

small $R_{F/N}^\downarrow$ for up spin
large $R_{F/N}^\uparrow$ for down spin → large MR ratios

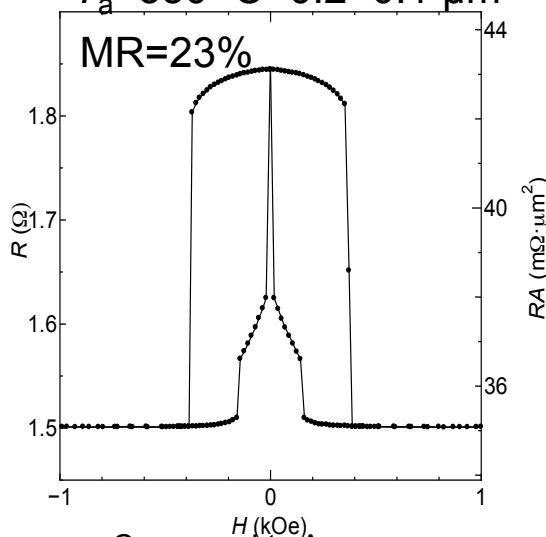
All B2 CPP-GMR



CFGG/CuZn/CFGG PSV

MgO/Cr(10)/Ag(100)/ $\text{Co}_2\text{FeGa}_{0.5}\text{Ge}_{0.5}$ (10)/CuZn(5)/ $\text{Co}_2\text{FeGa}_{0.5}\text{Ge}_{0.5}$ (10)/Ag(5)/Ru(8) (nm)

$T_a = 350$ °C 0.2×0.1 μm

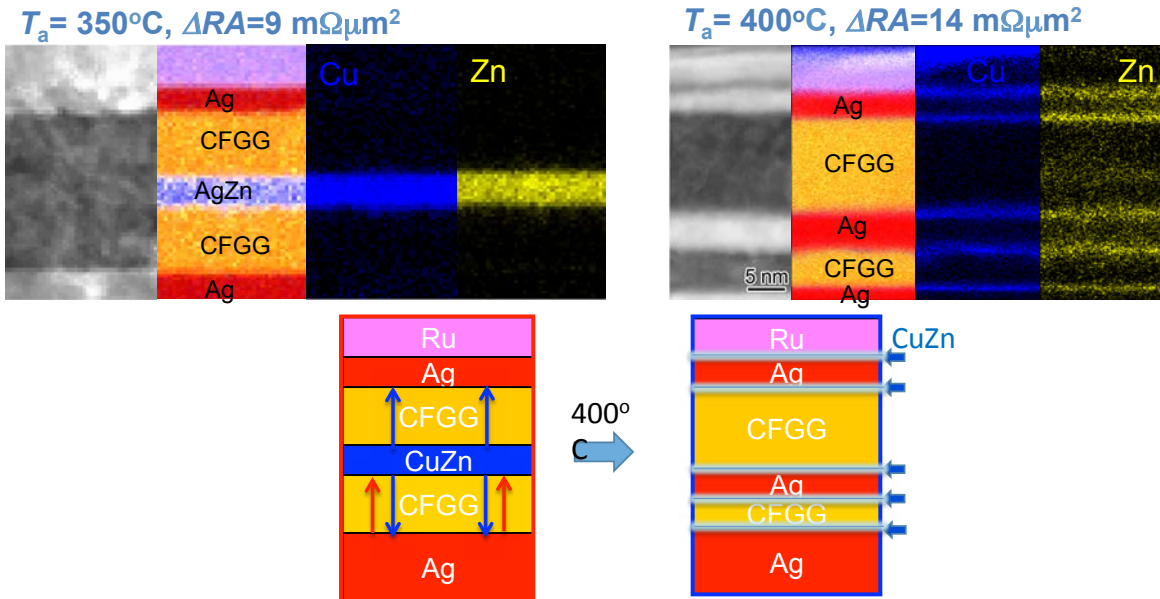


- Compared to Ag spacer*
 - larger $\Delta RA \sim 8 \text{ m}\Omega \cdot \mu\text{m}^2$ at low $T_a = 350$ °C
 - larger $R_p A \sim 35 \text{ m}\Omega \cdot \mu\text{m}^2 > \sim 20 \text{ m}\Omega \cdot \mu\text{m}^2$

*H.S. Goripati et al., J. Appl. Phys., 113. 043901 (2013).

T. Furubayashi et al. JAP, submitted.

Why CuZn spacer causes high ΔRA at low T_a ?



CuZn spacer is replaced with Ag spacer by interdiffusion!

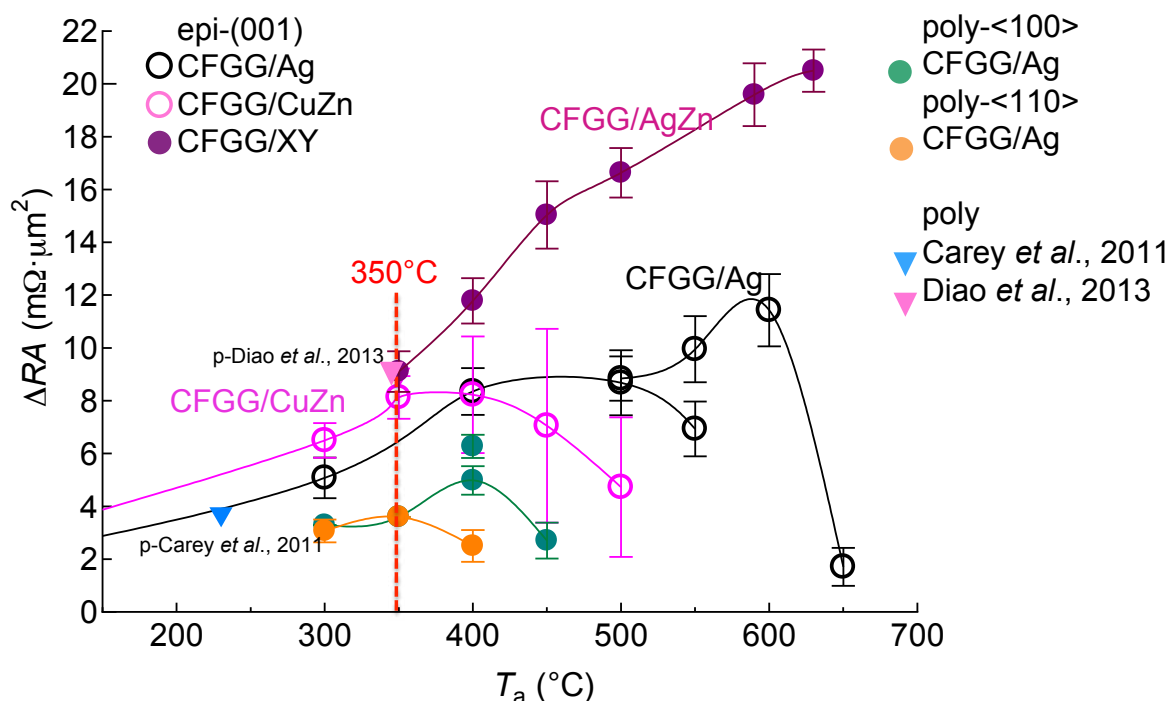
$$\Delta RA \approx 2\rho_F \frac{\beta^2}{1-\beta^2} t_F + 4A R_{F/N} \frac{\gamma^2}{1-\gamma^2}$$

- larger $R_p A$ compared to Ag space $\rightarrow R_{F/N} \uparrow$
- fast Zn diffusion may be responsible for high ΔRA at low T_a , 350°C

ΔRA and T_a of Heusler/NM/Heusler PSV



Du Ye



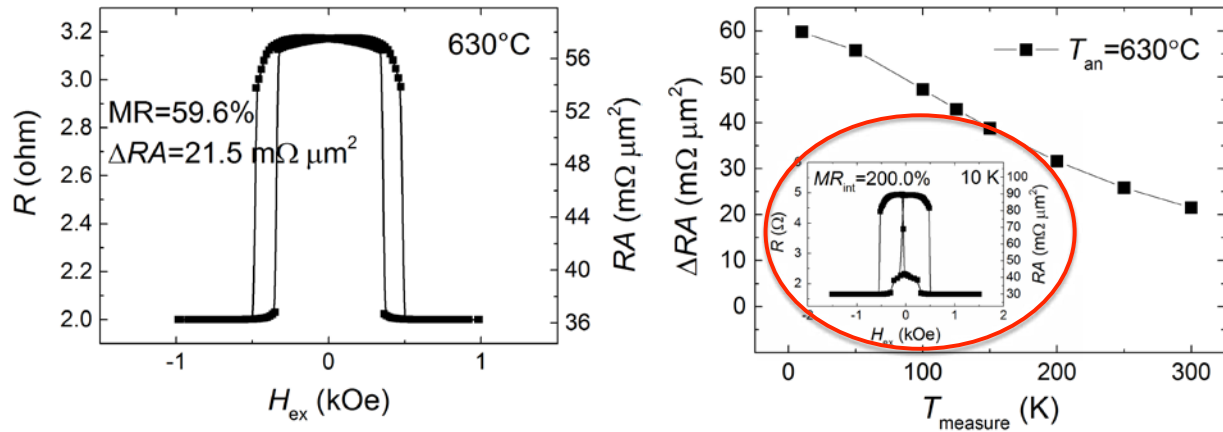
Y. Du et al. APL, submitted.

Very large ΔRA of CFGG/AgZn/CFGG PSV



MgO//Cr10/Ag100/CFGG10/AgZn5/CFGG10/Ag5/Ru8

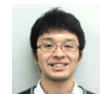
Du Ye



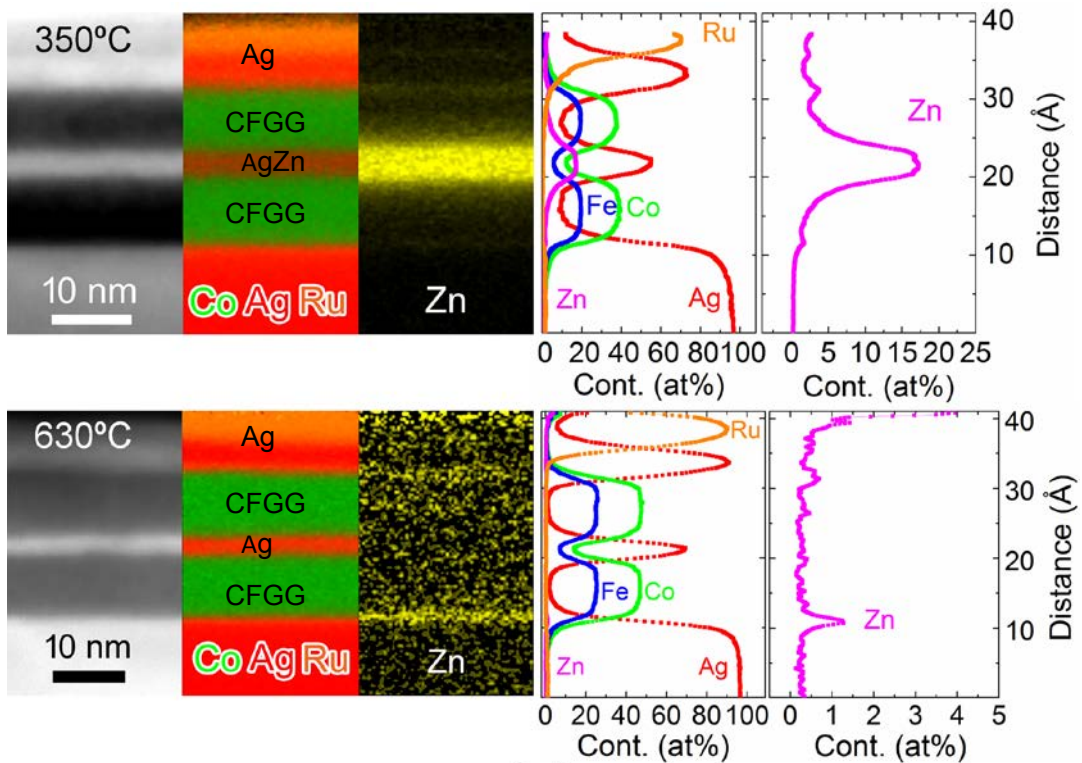
Selection of an appropriate spacer give large ΔRA – need of new materials search

Y. Du et al. APL, submitted.

Interlayer diffusion during annealing

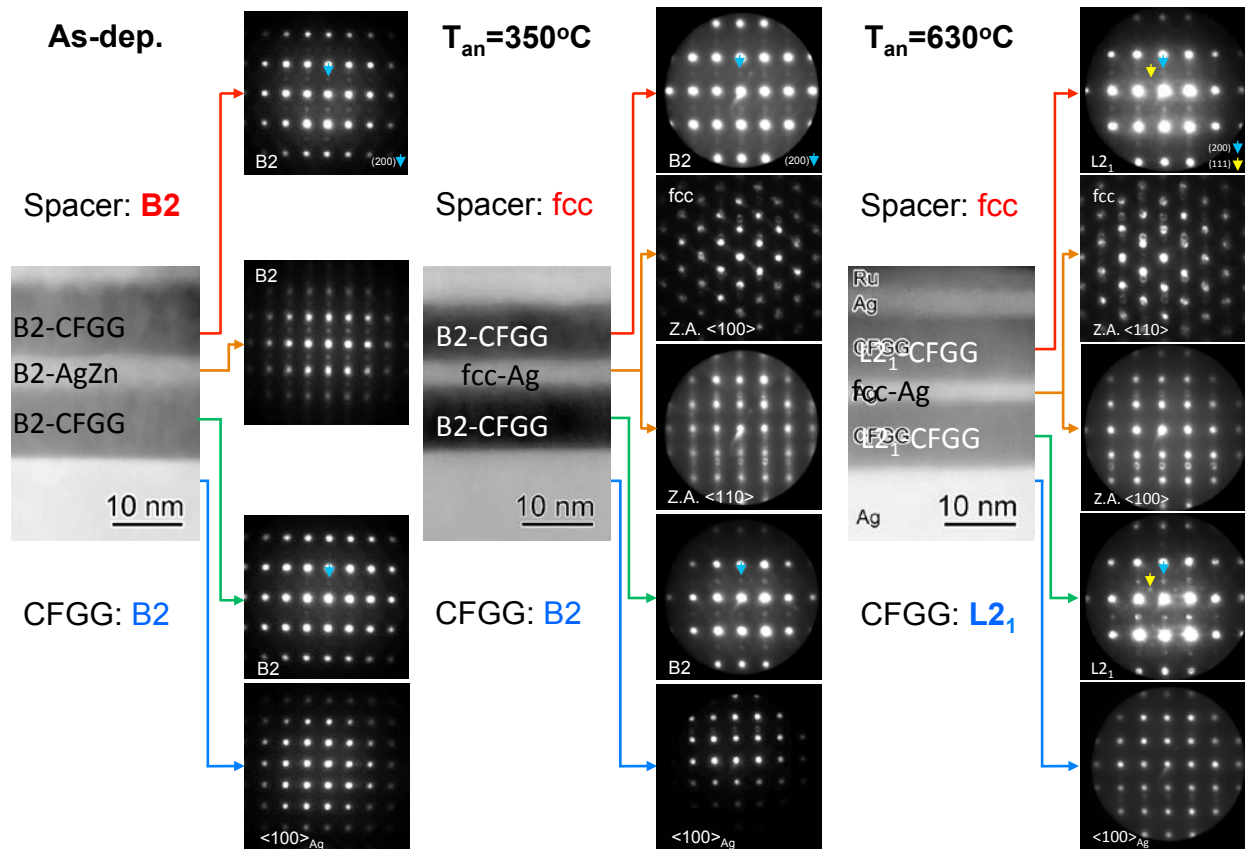


T. T. Sasaki



Y. Du et al. APL, submitted.

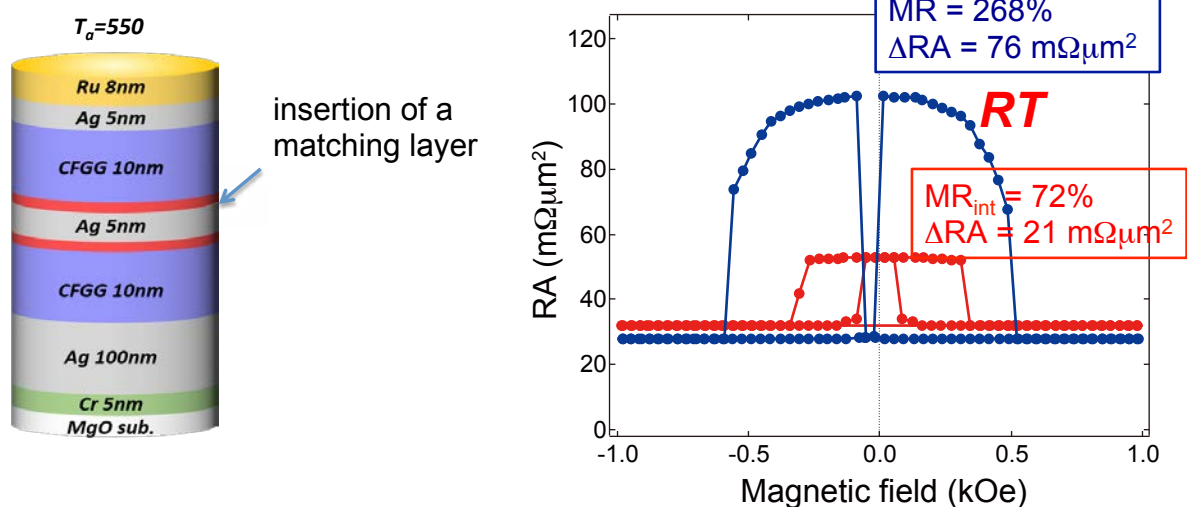
Structure of each layer in CFGG/XY/CFGG



268% GMR by interface band matching?

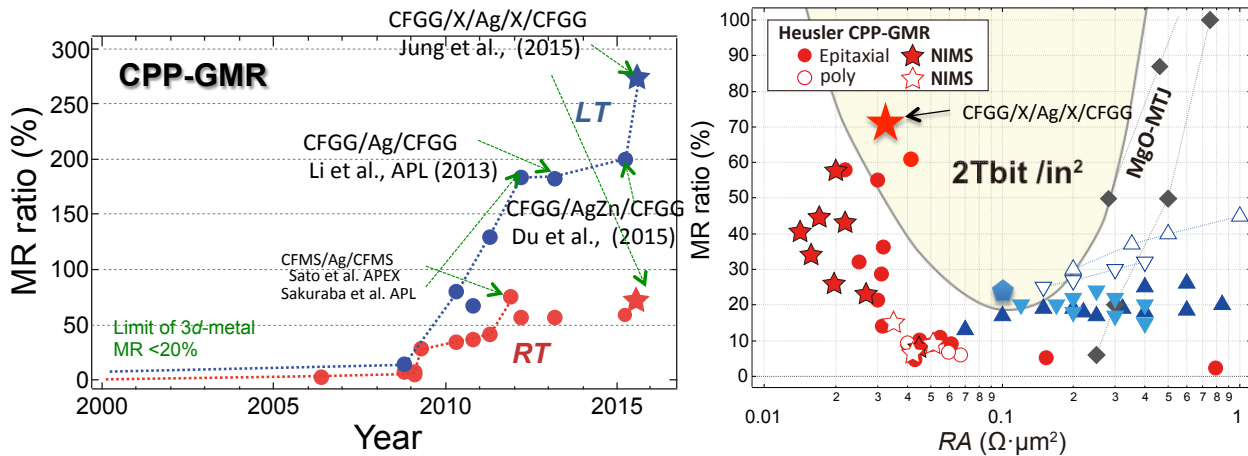


J. W. Jung



XY has an excellent band matching with Ag
 λ_s of XY is only ~2 nm → interface insertion

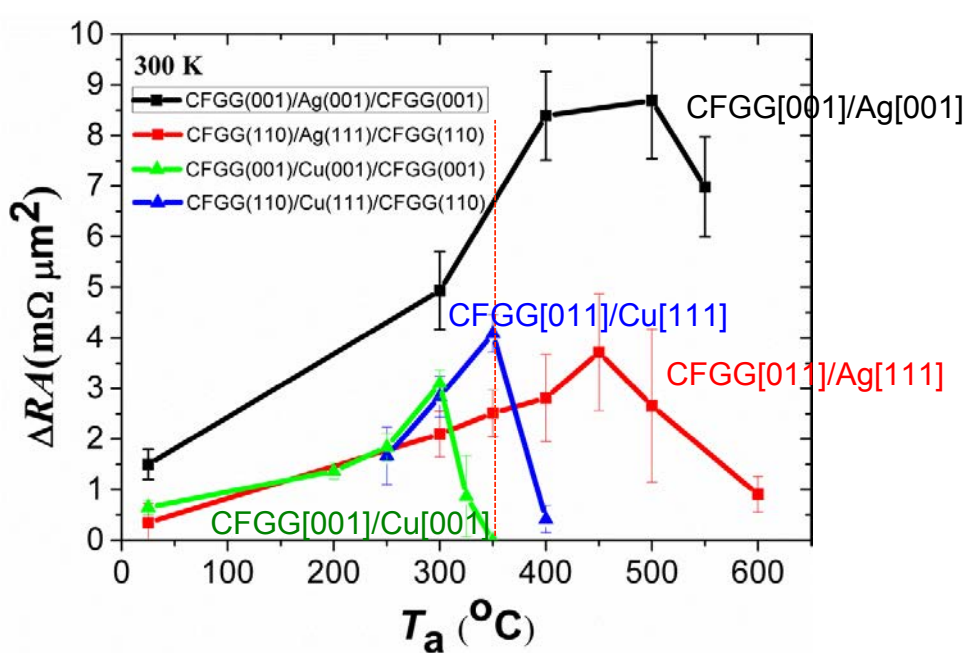
Heusler alloy based CPP-GMR



CFGG/Ag orientation dependence of ΔRA



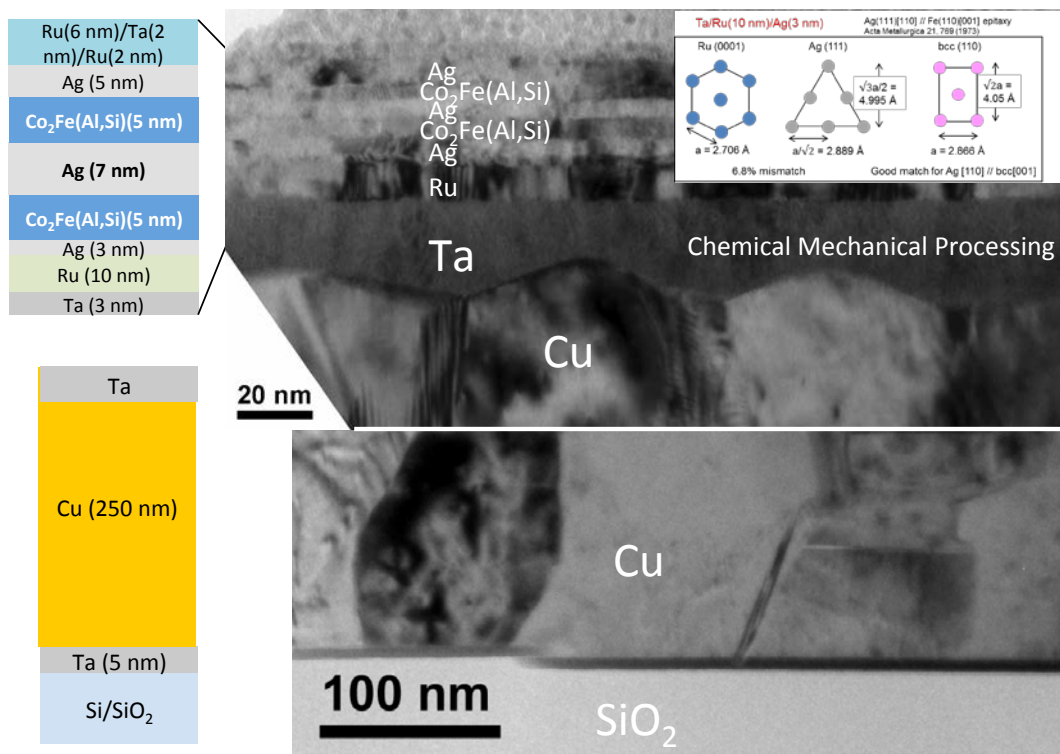
J. Chen



Polycrystalline CFAS PSV

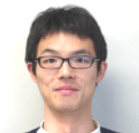


T. Nakatani

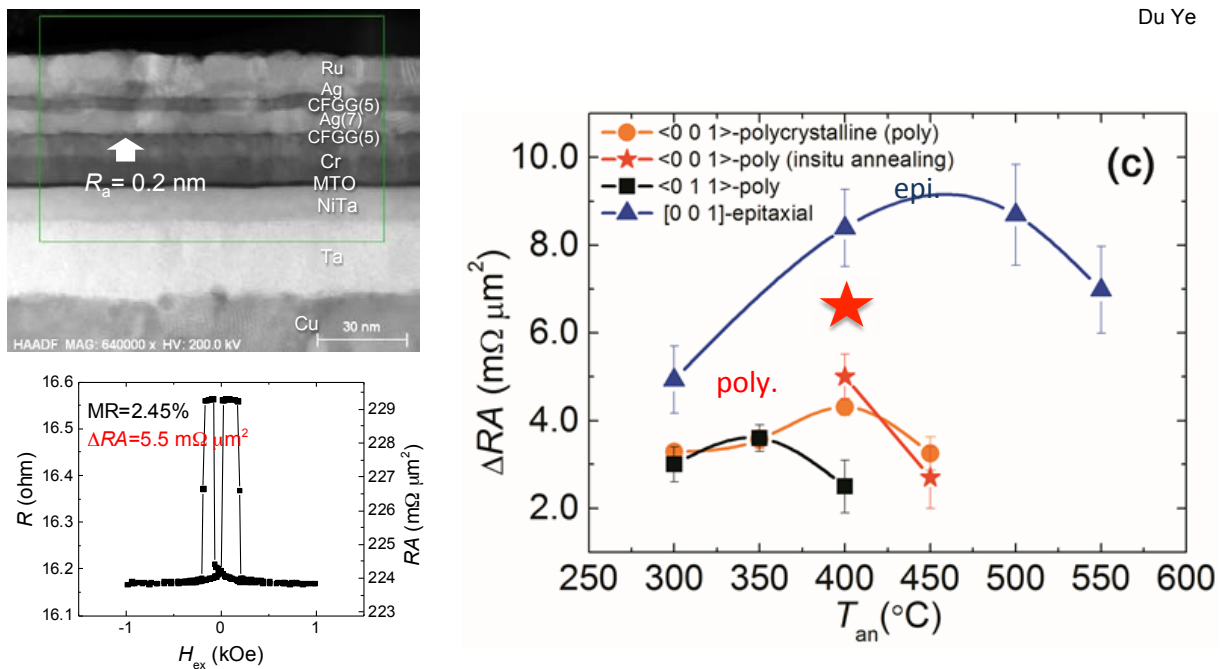


T.M. Nakatani et al. [Acta Mater. 61, 3695 \(2013\)](#).

(001) polycrystalline PSV: MTO buffer



Du Ye



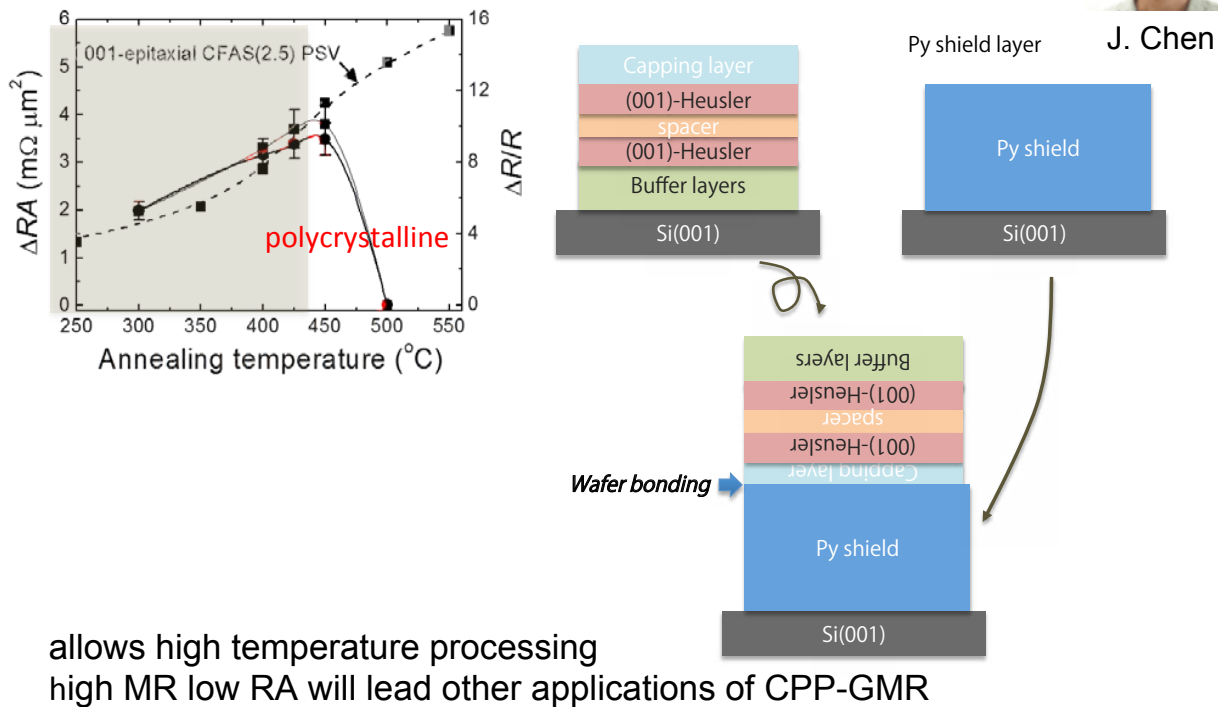
(001)-oriented device show higher DRA compared to (011)-oriented

Y. Du et al., APL 103, 202401 (2013).

Epitaxial device by wafer bonding



J. Chen

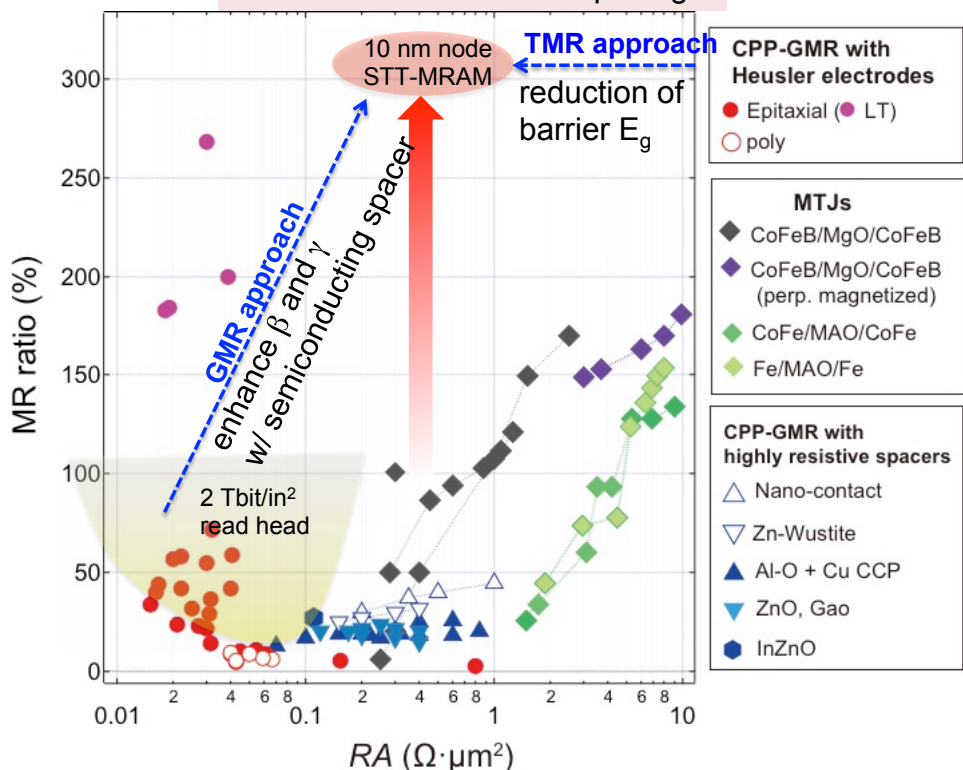


in collaboration with AIST



Future direction

MR>300%, RA<0.8 $\Omega \cdot \mu\text{m}^2$
for 10X STT-MRAM and spin-logic



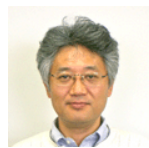
Acknowledgement



Y. Sakuraba



Y. K. Takahashi



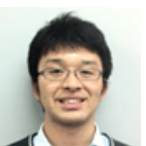
T. Furubayashi



S. T. Li



S. Bosu



T. T. Sasaki



J. W. Jung



T. Nakatani
(now HGST)



Ye Du



J. Chen



Ikhtiar

ASTC
ADVANCED STORAGE TECHNOLOGY CONSORTIUM

評新的研究開発推進プログラム
ImPACT
Impacting Paradigm Change through Disruptive Technologies Program